Analytica Chimica Acta 1180 (2021) 338858

Contents lists available at ScienceDirect

Analytica Chimica Acta

journal homepage: www.elsevier.com/locate/aca

# Enantioselective multiple heart cutting online two-dimensional liquid chromatography-mass spectrometry of all proteinogenic amino acids with second dimension chiral separations in one-minute time scales on a chiral tandem column

Ryan Karongo [a], Min Ge [a], Christian Geibel [a], Jeannie Horak [a, b, **], Michael Lämmerhofer [a, *]

[a] Institute of Pharmaceutical Sciences, Pharmaceutical (Bio-)Analysis, University of Tübingen, Auf der Morgenstelle 8, 72076, Tübingen, Germany
[b] Division of Metabolic and Nutritional Medicine, Dr. von Hauner Children's Hospital, Ludwig-Maximilians-University Munich Medical Center, Lindwurmstraße 4, 80337, Munich, Germany

## HIGHLIGHTS

- Multiple heart cutting 2D LC-MS for enantioselective amino acid (AA) analysis (AQC derivatized).
- $^{1}$D achiral RP separation of proteinogenic AAs and isobaric analogues of (aIle, Nle, Tle; Hse, aThr).
- $^{2}$D chiral separations of 24 amino acids achieved on a chiral tandem column in 68 s.
- Use of time-based sampling, smart peak parking and shifted gradient tool for efficient analysis.
- Fastest 2D-LC separation for enantioselective amino acid analysis to date (in total 45 min).

## GRAPHICAL ABSTRACT

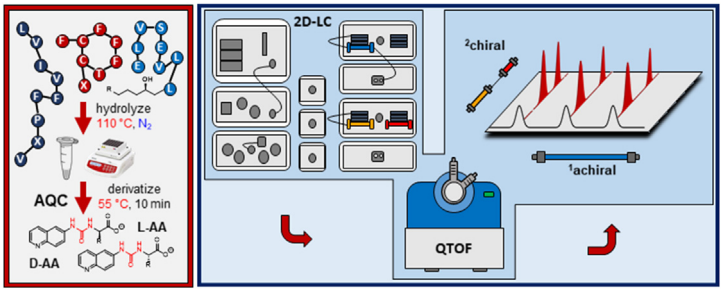


## ARTICLE INFO

*Article history:*
Received 7 June 2021
Received in revised form
15 July 2021
Accepted 16 July 2021
Available online 19 July 2021

*Keywords:*
Two-dimensional liquid chromatography
UHPLC
Multiple heart-cutting
Enantioselective amino acid separation
L-[u-$^{13}$C$^{15}$N] amino acid internal standard

## ABSTRACT

In this work, we present a unique, robust and fully automated analytical platform technology for the enantioselective amino acid analysis using a multiple heart cutting RPLC-enantio/stereoselective HPLC-ESI-QTOF-MS method. This 2D-LC method allows the full enantioselective separation of 20 proteinogenic AAs plus 5 isobaric analogues, namely *allo*-Threonine (aThr), homoserine (Hse), *allo*-isoleucine (alle), *tert*-Leucine (Tle) and Norleucine (Nle), after pre-column derivatization with 6-aminoquinolyl-*N*-hydroxysuccinimidyl carbamate (AQC; AccQ). This N-terminal AA-derivatization method introduces on the one hand beneficial chromatographic properties for $^{1}$D RP-LC (stronger retention) and $^{2}$D chiral separation (better chiral recognition), and on the other hand favorable detection properties with its chromophoric, fluorophoric, and easily ionizable quinoline mass tag. The entire separation occurs within a total 2DLC run time of 45 min, which includes the $^{1}$D-RP run and the 68 s $^{2}$D chiral separations of 30 heart-cuts (from the $^{1}$D-RP-run) on a chiral quinine carbamate (core-shell QNAX/fully porous ZWIX) tandem column. This relatively short overall run time was only possible by utilizing the highly efficient "smart peak parking" algorithm for the heart cuts and the resulting optimized analysis order thereof. $^{1}$D

* Corresponding author. Pharmaceutical (Bio-)Analysis, Institute of Pharmaceutical Sciences, University of Tübingen, Auf der Morgenstelle 8, 72076, Tübingen, Germany.
** Corresponding author. Division of Metabolic and Nutritional Medicine, Dr. von Hauner Children's Hospital Ludwig-Maximilians-University, Munich Medical Center, Lindwurmstraße 4, 80337, Munich, Germany.
*E-mail addresses:* Jeannie.Horak@med.uni-muenchen.de (J. Horak), michael.laemmerhofer@uni-tuebingen.de (M. Lämmerhofer).

https://doi.org/10.1016/j.aca.2021.338858
0003-2670/© 2021 Elsevier B.V. All rights reserved.

6-Aminoquinolyl-*N*-Hydroxysuccinimidyl carbamate

retention time precisions of <0.21% RSD were a requirement for the time-based sampling mode and finally led to a robust, fully automated enantioselective amino acid analysis platform.

This achiral-chiral 2DLC method was applied for the amino acid stereoconfiguration assignment of three peptides (aureobasidin A, a lipopeptide research sample, and octreotide) using an L-[u-$^{13}C^{15}N$] labelled internal AA standard mix spiked to each sample. The isotopically labelled L-AA standard allowed an easy and straightforward identification and configuration assignment, as well as the relative quantification of amino acids within the investigated peptides, allowing the direct determination of the number of respective amino acids and their chirality within a peptide.

© 2021 Elsevier B.V. All rights reserved.

**Abbreviations**

| | |
|---|---|
| aThr | *allo*-Threonine |
| Hse | homoserine |
| aIle | *allo*-isoleucine |
| Nle | norleucine |
| Tle | *tert*-leucine |
| AQC;AccQ | aminoquinolyl-*N*-hydroxysuccinimidyl carbamate |
| AA | amino acid |
| OPA | *ortho*-phthaldialdehyde |
| MHC | multiple heart-cutting |
| mLC-LC | multiple heart-cutting two-dimensional liquid chromatography |
| IDA | information dependent acquisition |
| FLD | fluorescence detection |
| CSP | chiral stationary phase |
| QN-AX | quinine-carbamate-based anion-exchanger CSP |
| ZWIX | zwitterionic quinine-carbamate-based CSP |
| WAX | weak anion exchange |
| SCX | strong cation exchange |
| SPP | superficially porous particles (core-shell) |
| FPP | fully porous particles |

## 1. Introduction

For many decades, homochirality (L-configuration of amino acids) had been considered the norm in nature, but with the gradual discoveries of D-AAs in various biological matrices, as free D-AAs as well as incorporated in peptides, awareness has been aroused towards their stereochemical consequences in bioactivity. Therefore, the interest in determining D-amino acids in biochemical environments such as tissues and physiological fluids is continuously increasing, especially since they have been related to various diseases, e.g. D-Asp and D-Ser in age related disorders such as cataract [1], multiple sclerosis [2] and Alzheimer's disease [3]. On the other hand, peptides are increasingly emerging as therapeutical agents, whereby the enantiomeric purity of each amino acid within the peptide is crucial, especially for those derived from synthesis [4]. On the other hand, non-ribosomal peptides produced by microorganisms, such as lipopeptides, are raising great interest as potential novel bioactive peptides. Their structure often contains D-amino acid enantiomers and frequently non-proteinogenic AAs such as alle, aThr, and Hse, amongst many others [5].

For a long time, direct enantioselective gas chromatography on Chirasil Val using *N*- and *C*-terminal amino acid derivatization [5–8] or indirect chiral liquid chromatography (LC) on reversed phase columns using chiral derivatizing agents such as *ortho*-phthaldialdehyde (OPA) and chiral thiols [9] or Marfey's reagent [10–12] have been employed as first choice for chiral separation [13]. In the last decades, however, direct LC approaches using chiral stationary phases have become more popular for the analysis of complex amino acid enantiomer mixtures [11], allowing chiral separation of underivatized AAs [17] as well as achiral precolumn derivatization followed by mass spectrometric detection [14–17]. Common examples for achiral precolumn derivatization supporting chiral separation comprise 6-aminoquinolyl-*N*-hydroxysuccinimidyl carbamate (AQC) [18,19], 1-fluoro-2,4-dinitrobenzene (DNB-F, Sanger's reagent) [20], 4-fluoro-7-nitro-2,1,3-benzoxadiazol (NBD) [21], dansyl chloride (Dns) [22,23] and 9-fluorenylmethyl-chloroformate (Fmoc-Cl) [24–26]. Innovative approaches to analyze AAs comprise SFC [27], ion mobility mass spectrometry [28,29] and 2D-LC [25,30–33].

Many of these one-dimensional methods can separate the majority of amino acid enantiomers, but fail for the one or the other amino acid. One particular problem is the separation of the isobaric amino acids with isomeric side chains (e.g. Leu, Ile, alle) or the secondary amino acids (like Pro). 2D-LC with achiral pre-separation can resolve some of these selectivity issues in complex samples and issues with interferences and matrix effects [30]. Although technically still challenging, the recent decade has experienced a great technological leap in multidimensional chromatography and

brought about commercially available, highly robust 2D-LC systems. This has triggered various endeavors to improve peak capacity, selectivity, resolving power, separation time etc. by establishing 2D-LC methods, despite the complex method development necessary to combine chromatographic parameters across multi-dimensional systems [30,34–39].

A special mode in 2D-LC analysis is multiple heart-cutting (MHC), in which multiple peaks or fractions thereof which contain the analyte/s of interest are transferred from the first dimension ($^1$D) to the second dimension ($^2$D) and then separated by a second complementary chromatographic principle [40,41]. Desirably, 2D-LC methods should exhibit a maximum extent of orthogonality between both dimensions, which is achievable when each of them targets a specific sample dimensionality (e.g. hydrophobicity in the $^1$D and chirality in the $^2$D, or vice versa).

MHC for AAs has been applied by Ianni et al. [22], Ishii et al. [21] and Woiwode et al. [42] using an achiral (RPLC) - chiral 2D-LC system after pre-column derivatization with either dansyl chloride, NBD-F and Sangers reagent, respectively. These reagents not only increase detectability, but also the RPLC retention of otherwise very hydrophilic amino acids. While tagging can improve electrospray ionization efficiency and detection sensitivity, even with HRMS the chromatographic resolution of isobaric amino acids is mandatory, especially the leucine analogues with alle being especially problematic. Woiwode et al. were able to separate all proteinogenic amino acids in one run (130 min) except for the isobaric analogues of Leu, which were only partially resolved, but enough to get clean cuts [42]. Hamase and coworkers usually select a set of biologically relevant amino acids, and their 2DLC as well as 3DLC separations have usually long analysis times (>2 h) [21,30].

The present study is focused on the establishment of a robust, fully automated online MHC achiral-chiral 2D-LC method using RPLC in the $^1$D and cinchona alkaloid-derived ion-exchange type chiral stationary phases [43] in the $^2$D for the analysis of AQC-derivatized AAs, which can accomplish the full separation in less than an hour. Chemoselective derivatization is a common strategy in amino acid analysis, for both achiral and chiral approaches. The advantages for the current chiral separation are manifold. It increases retention and selectivity of polar amino acids in RPLC, provides them with favorable functional groups tunable for effective chiral recognition process of the utilized chiral stationary phase (CSP), drives the relative enantiomer affinity towards the chiral selector and thus determines the elution order, and last but not least allows the introduction of chromophoric, fluorophoric, electrochemical and better ionizable mass tags for sensitive UV, fluorescence, electrochemical or MS detection.

Numerous derivatization reagents have been successfully tested and employed for the LC enantiomer separation on cinchonan carbamate based CSPs [44], including arylhalides such as Sanger's reagent [20,45], NBD-F [46–48], chloroformates or corresponding OSu derivatives such as FMOC-Cl/-OSu [25,49], acyl chlorides like benzoylchlorides [50,51], and AQC [19,52]. Precolumn derivatization of amino acids with 6-aminoquinolyl-*N*-hydroxysuccinimidyl carbamate (AQC) followed by reversed phase HPLC separation with fluorometric detection is a method suggested by pharmacopeias which makes it an attractive choice for $^1$D separation. AQC combines favorable detection characteristics, possessing a strong quinoline chromophore for UV detection, which is also a fluorophore allowing highly sensitive fluorescence detection (FLD) ($\lambda_{Ex}$ 250, $\lambda_{Em}$ 395 nm) reaching LODs at the fmol level [12], but representing also a favorable mass tag with excellent ionization efficiencies in positive ion mode for the negatively charged AQC-amino acid derivatives. Its fast reaction kinetics allows derivatization at 55 °C in 10 min. Moreover, D/L mixtures of [u-$^{13}$C$^{15}$N] amino acid internal standards are accessible by a simple protocol from commercially available L-[u-$^{13}$C$^{15}$N]-AA IS mix [18]. The stable isotope labelled D/L-internal standard mixture facilitates identification and allows corrections for (enantioselective) matrix effects when utilizing MS detection. Thus, in the current study, a standard mix of all proteinogenic amino acids, including the five isobaric analogues Hse, aThr, Tle, alle and Nle was prepared for method development and was additionally spiked with an L-[u-$^{13}$C$^{15}$N] amino acid IS standard mixture for L-enantiomer identification.

Particular focus was set on the resolution of all AAs with emphasis on the isobaric analogues (Thr, aThr, Hse and Leu, Ile, alle, Tle, Nle) for which neither MS nor the $^2$D chiral separation has enough selectivity. Furthermore, for time-based sampling procedure excellent run-to-run repeatabilities are required for the $^1$D RPLC separation and method optimization was carried out in consideration of this demand. An additional challenge was the complete enantioselective separation of all 24 chiral AA pairs within a reasonable timeframe on one chiral column in the $^2$D to accommodate the complete analysis of all heart cuts. By the virtue of mass spectrometric detection, the separation of non-isobaric AAs in the $^1$D was not critical. Chiral separation of all amino acids was finally achieved by a tandem setup with a core-shell *tert*-butyl carbamate modified quinine based chiral stationary phase (QN-AX) followed by a short zwitterionic quinine type stationary phase (Chiralpak ZWIX(+)) [15,53,54]. The applicability of the automated 2D-LC setup is demonstrated by the amino acid configuration determination of three peptides.

## 2. Materials and methods

### 2.1. Materials

Acetonitrile, methanol and formic acid (FA) purchased from Carl Roth (Karlsruhe, Germany) were of ultra-LC–MS grade quality. All amino acids (AAs), ammonium formate ($NH_4FA$), hydrochloric acid (HCl), dithiothreitol (DTT), deuterium oxide, deuterium chloride, boric acid, sodium hydroxide, iodoacetamide (IAA) were provided by Sigma Aldrich, Schnelldorf (Germany). A solution of uniformly labelled [u-$^{13}$C$^{15}$N] L-amino acid metabolomics standard mix (2.5 mM in 0.1 M HCl) which contained all labelled proteinogenic amino acids with exception of asparagine, glutamine and tryptophan was acquired from Euroisotop GmbH (Saarbrücken, Germany) and was used as internal standard. Single L- or DL-amino acid stock solutions (50 mM in 0.1 M HCl) were used to prepare a 2.5 mM stock solution. All amino acid standard solutions were stored at −20 °C prior to use. Water was purified using a Water Purelab Analytics Purification System from ELGA (Celle, Germany). 6-Aminoquinolyl-*N*-hydroxysuccinimidyl carbamate (AQC, AccQ) was purchased from Synchem (Felsberg/Altenburg, Germany). Derivatization reactions were performed in 1.5 mL Crystal Clear microcentrifuge tubes from Starlab (Hamburg, Germany) using a Thermo-Shaker PHMT Gant-bio for 1.5 mL micro-centrifugation tubes (PSC24 N) from Grant Instruments Ltd. (Shepreth, England).

For achiral chromatographic separations a ZORBAX SB-C18 (1 × 50 mm, 3.5 μm) from Agilent Technologies (Waldbronn, Germany), an Acquity UPLC BEH C18 (1 × 150 mm, 1.7 μm) and an

XBridge BEH C18 (1 × 150 mm, 3.5 μm), both from Waters (Eschborn, Germany), were used. For preliminary MHC-2D-LC experiments, a core-shell QN-AX column (3 × 50 mm, 2.7 μm, 160 Å) [54] was tested.

For the final optimized method, however, a self-made chiral QNAX-ZWIX tandem column consisting of a core-shell QN-AX column (3 × 50 mm, 2.7 μm, 160 Å) [54] coupled to an in-house packed Chiralpak ZWIX(+) FPP (3 × 20 mm, 3.0 μm) [53,55] column using a short stainless steel capillary (0.12 mm id, 75 mm) was employed.

### 2.2. Sample preparation

For peptide hydrolysis the sample was dissolved in 1 mL of 6 M DCl in $D_2O$ (1 mg $mL^{-1}$). The glass vial was sealed under nitrogen and heat-treated at 110 °C for 16 h. Subsequently, the sample was evaporated to dryness, the residue re-dissolved to the original volume (1 mL) with 0.4 M borate buffer (pH 8.8), vortexed, and centrifuged for 60 s at 13,200 rpm. The supernatant was used for AQC derivatization of the liberated amino acids.

Non-isotopically labelled AA stock solutions (L-[u-$^{12}C^{14}N$]-amino acids) as standard mixtures were prepared at a concentration of 2.5 mM in 0.1 M HCl containing all proteinogenic amino acids and additionally Hse, aThr, alle, Tle and Nle as isobaric analogues.

#### 2.2.1. Alkylation

Cysteine-containing mixtures were prepared according to the following protocol [14,18]. Iodoacetamide (IAA) and dithiothreitol (DTT) were freshly prepared at a concentration of 10 mM in ultrapure water shortly before use and kept on ice. Solutions of 10 μL AA mix (2.5 mM), 5 μL DTT and 10 μL L-[u-$^{13}C^{15}N$]-AA IS (0.25 mM) were added to a solution of 40 μL 0.4 M sodium borate buffer (pH 8.8) in a 1.5 mL microcentrifuge tube. The reaction solution was placed on a thermoshaker (Grand Instruments) and allowed to react at 800 rpm and 55 °C for 10 min. After short centrifugation (13200 rpm, 4 °C, 1 min), 10 μL IAA was added followed by heating (55 °C) and shaking (800 rpm) for 10 min. After centrifugation, 5 μL DTT were added followed by yet another step of heating and shaking. Subsequently, 40 μL of this solution was filled up to 50 μL with ultrapure water (0.25 mM AA mix-IAA). For direct MS measurements, the solution was further diluted 1:10 with 0.4 M sodium borate buffer (pH 8.8) prior to derivatization with AQC reagent.

#### 2.2.2. Derivatization

The derivatization reagent AQC was prepared at a concentration of 3 mg $mL^{-1}$ in dry acetonitrile (AQC: 10.5 mM), stored at −20 °C and shortly ultrasonicated before use. If not otherwise stated 10 μL sample solution (0.25 mM AA mix or hydrolyzed sample) was added to 80 μL 0.4 M sodium borate buffer (pH 8.8), followed by the addition of 10 μL AQC reagent solution. This reaction solution was immediately heated to 55 °C for 10 min at 800 rpm. After centrifugation the sample was ready to use. According to the European Pharmacopoeia 10.0 peak areas for AQC-amino acids remain unchanged for at least a week at room temperature. Nevertheless, the samples were constantly cooled in the autosampler at 4 °C and were only utilized for a week, then freshly prepared.

### 2.3. Instrumentation

An Agilent 1290 Infinity II 2D-LC Solution from Agilent Technologies (Waldbronn, Germany) was used for multiple heart-cutting 2D-LC (Suppl. Fig. S1). The $^1$D LC consisted of a quaternary low pressure gradient UHPLC pump (Flexible Pump, G7104A), a Multisampler (G7167B), a Multicolumn Thermostat (G7116B), a diode array detector (G7117B) with 1 μL flow cell (#G4212-60008) and a pressure release kit (G4236-60010) between UV-detector and 2D-interface. The $^2$D comprised a binary high-pressure gradient UHPLC pump (High Speed Pump, G7120A), a valve drive (G1170A) with a 5 position/10 port 2D-LC active solvent modulation (ASM) valve (5067–4266) connected to two 6 position/14 port valve heads (5067–4142) carrying six 40 μL loops each and a multicolumn thermostat (G7116B). Experiments utilizing active solvent modulation (ASM) were performed with the ASM factor 5 (split ratio 1:4) restriction capillary (85 × 0.12 mm, 0.96 μL). For enhanced detection, a QuickSplit Flow Splitter from ERC (Riemerling, Germany) was installed prior to the detectors in the $^2$D at a ratio of 1:5, whereby the high flow was directed to a variable wavelength detector (VWD) (G7114B) with a 2 μL (initially 14 μL) flow cell (G1314-60187) connected in series with a fluorescence detector (FLD) (G1321A) with an 8 μL flow cell (standard FLD cell) and the low flow to a TripleTOF 5600+ QTOF mass spectrometer from Sciex (Concord, Ontario, Canada) using a contact closure connection for peripheral devices. The acquisition rates were set to 10 Hz in the $^1$D for the DAD, and 20 and 18.52 Hz for VWD and FLD detectors in the $^2$D, respectively. Dwell volumes were determined using a zero dead volume union connector in place of the column. The measured dwell volumes were 550 μL in the $^1$D and 120 μL in the $^2$D at a flow rate of 0.20 mL $min^{-1}$. The 2D-chromatographic data were processed with Open Lab CDS Rev. C.01.07 SR4 from Agilent Technologies (Waldbronn, Germany) and DryLab 4 software (Molnár-Institute, Germany).

The optimization of the $^2$D chiral separation was performed on an Agilent 1290 UHPLC system with a 1290 binary pump (G4220A), a 1290 thermostated column oven (G1316C), a Sciex calibrant delivery system (CDS) for calibration (Waldbronn, Germany) and a CTC-PAL HTS autosampler from CTC Analytics (Zwingen, Switzerland).

QTOF-MS measurements were performed using a Duospray ion source operated in positive electrospray ionization mode. The following MS instrument parameters were used: curtain gas (CUR) 40 psi, ion source gas (nebulizing gas; GS1) 60 psi, heater gas (drying gas; GS2) 60 psi, ion spray voltage floating (ISVF) 5500 V, source temperature (TEM) 400 °C and declustering potential (DP) 100 V. Data acquisition was performed in information-dependent acquisition (IDA) in high sensitivity mode with an inclusion list comprising the *m/z* ratios of the precursor ions of all single and double derivatized amino acid compounds (Table S2). The mass range of the TOF-MS full scan comprised *m/z* 30–2000 with an accumulation time of 250 ms and a collision energy (CE) of 10 V. MS/MS in IDA (top 4) was performed with 45 V CE and 15 V CE spread (CES) and an accumulation time of 100 ms. Mass calibration was conducted with a calibrant delivery system (Sciex, Darmstadt, Germany) through the APCI inlet using the positive calibration solution for the SCIEX X500 System. Data acquisition and analysis was performed with Analyst TF 1.7 and PeakView software (Sciex), respectively. Chromatographic conditions are specified in the respective figure captions.

## 3. Results and discussion

### 3.1. Optimization of $^1$D for AA analysis

Several critical factors need to be considered for the $^1$D method development, including sufficient resolution between critical peaks that cannot be resolved in the $^2$D or by MS detection, mobile phase compatibility between $^1$D and $^2$D, run-to-run repeatability, and gradient-dwell volume as well as extra-column peak broadening effects. The AQC amino acid method stated in the European Pharmacopoeia (Ph. Eur.) 10th Edition exhibits full resolution of amino

acids including Ile and Leu. However, other isobaric amino acids often present in microbial lipopeptides like alle, aThr, Hse are not considered. Their simultaneous achiral separation in the presence of all the other proteinogenic amino acids pose a major challenge for the $^{1}$D RPLC-UV or -FLD method.

Initially three distinct mobile phase compositions were investigated on a Zorbax SB-RP (50 × 1.0 mm, 3.5 μm) containing water with 10 mM $NH_4FA$ or 10 mM $NH_4FA$ and 10 mM FA or 0.05% (v/v) FA as mobile phase A (MP-A) and ACN as MP-B (Fig. S2). Despite an efficient separation of most amino acids, the critical isobaric pair of Ile and alle was not even partially separated. Consequently, the column was replaced by an Acquity UPLC BEH C18 (1 × 150 mm, 1.7 μm) column. Acidic analytes like AQC-amino acids exhibit stronger retention and good peak shapes with 0.1% TFA as additive. However, TFA was avoided for incompatibility reasons with the $^{2}$D as it represents a strong counterion for the anion exchange selector in the $^{2}$D chiral separation with quinine-type CSPs. Therefore, FA at 0.05% (v/v) as a weaker acid and counterion was deemed appropriate for the compatibility between the $^{1}$D and $^{2}$D. Furthermore, it was found that methanol improved the peak shapes for the early eluting amino acids, while ACN was more beneficial for the late eluting AAs. Consequently, a low percentage (1%, v/v) of MeOH was added to the aqueous MP-A, while ACN without additives was used as MP-B. As a result, all isobaric amino acids, namely Thr, aThr and Hse as well as Ile, alle, Leu, Nle and Tle could be resolved from each other (Fig. S3). A further improvement of resolution and peak shape was achieved by elevating the temperature from 30 to 50 °C, especially for Met (9) and Tyr (12), Ile (8) and alle (23), respectively

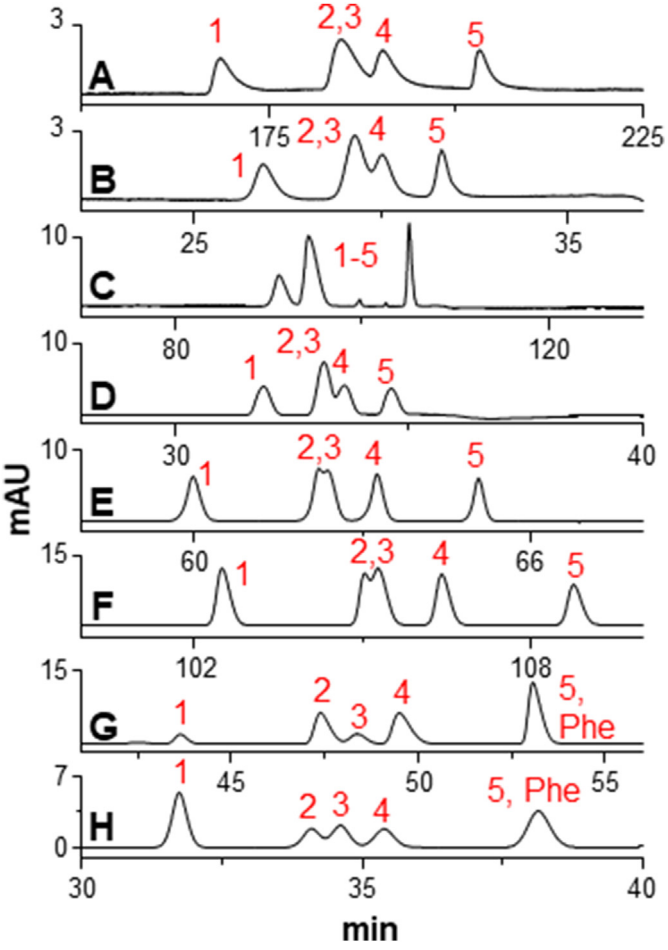


**Fig. 1.** Chromatographic separation of *tert*-Leucine (1), Isoleucine (2), *allo*-Isoleucine (3), Leucine (4), Norleucine (5) recorded on a variety of columns in under reversed phase conditions using **MP-A:** 0.05% FA + 1% MeOH in water and **MP-B:** 0.05% FA in ACN. Columns: **A**: COSMOSIL Cholester (250 × 4.6 mm, 2.6 μm), **B**: Cortecs C18+ (50 × 2.1 mm, 2.7 μm), **C**: COSMOCORE PBr (150 × 2.1 mm, 2.6 μm), **D**: Gemini C18 (100 × 1.0 mm, 3 μm), **E**: Kinetex C18 (100 × 3.0 mm, 2.6 μm), **F**: Poroshell EC C18 (150 × 3.0 mm, 2.7 μm), **G**: Acquity BEH C18 (150 × 1.0 mm, 1.7 μm), **H**: XBridge BEH C18 (150 × 1.0 mm, 3.5 μm). Method transfers were executed for each column proceeding from the Acquity BEH C18 according to 0.5 μL injection volume, 0.15 mL $min^{-1}$ flow rate and the following gradient: 0–2.15 min − 0 %B, 2.15–24.65 min − 0-7.5 %B, 24.65–35.90 min − 7.5 %B, 35.90–47.15 min − 7.5–15 %B, 47.15–48.65 min − 15–50 %B, 48.65–51 min − 50 %B, 51–51.10 min − 50-0 %B, 50–65 min − 0 %B.

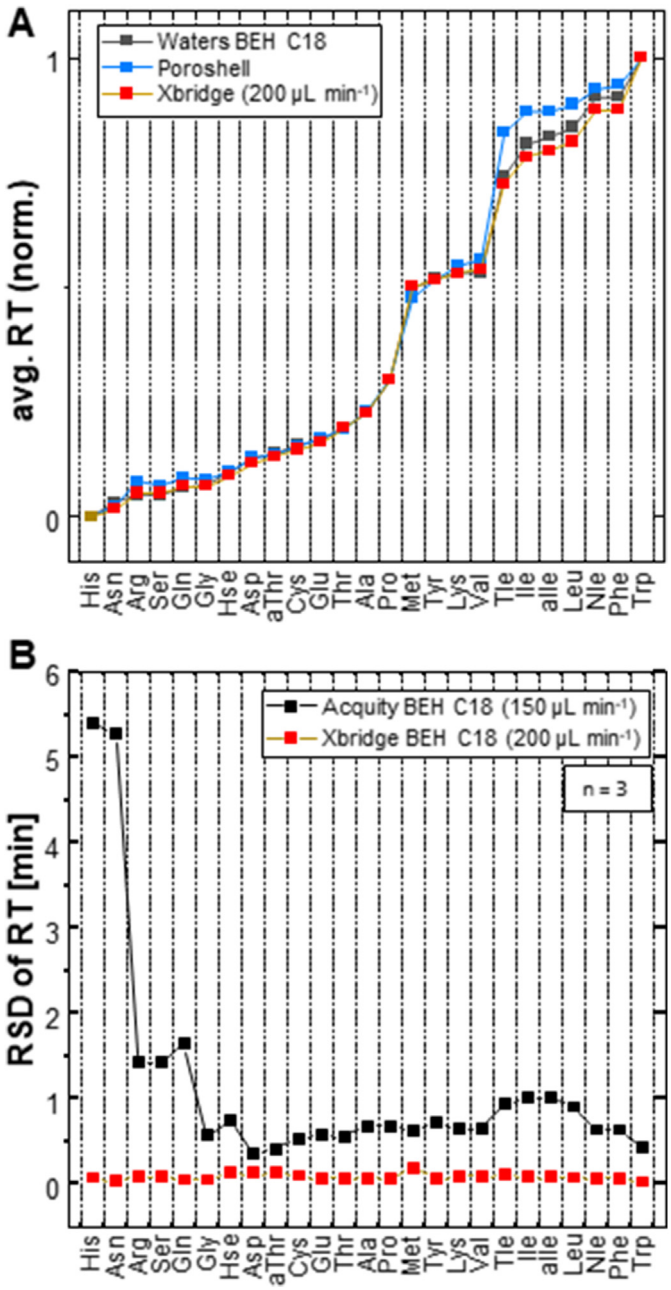


**Fig. 2.** A) Normalized retention times for 25 amino acids between the first and last eluting compounds were recorded on the following stationary phases: Acquity BEH C18 (150 × 1.0 mm, 1.7 μm), XBridge BEH C18 (150 × 1.0 mm, 3.5 μm) and Poroshell EC C18 (150 × 3.0 mm, 2.7 μm) according to the method conditions described in Fig. 1. B) RSDs (n = 3) of 25 AAs were calculated on the Acquity BEH C18 (150 × 1.0 mm, 1.7 μm) and XBridge BEH C18 (150 × 1.0 mm, 3.5 μm) at 150 μL $min^{-1}$ and 200 μL $min^{-1}$, respectively.

(Fig. S4). Although a flow rate of 0.07 mL $min^{-1}$ was applied for method development, it was increased to 0.15 mL $min^{-1}$ in order to stabilize run-to-run repeatability and reduce relative standard deviations of retention times across consecutive chromatograms (Fig. S5), which is a critical factor for time-based MHC 2D-LC. However, this improvement of repeatability was achieved at the expense of resolution for the early eluting AA pairs Arg/Ser, Gln/Gly, Val/Lys. Nle and Phe could not be resolved whichever flow rate was used. Since they are not isobaric they can be distinguished by MS detection. Finally, a DryLab optimization was performed to finalize method development for the $^{1}$D resulting in a step gradient (step gradient 2, Fig. S6), which was used for further experiments [56].

In order to establish a successful time-based multiple heart-cutting method, the $^{1}$D retention times have to be highly reproducible with a run-to-run repeatability of <0.5% RSD. The necessity of a time-based method will be discussed in chapter 3.4. The Acquity UPLC BEH (150 × 1.0 mm, 1.7 μm) column proved the necessary selectivity to successfully separate the isobaric compounds Tle, Ile, alle, Leu and Nle, as shown above. However, the high backpressure generated by the 150 mm long column packed with 1.7 μm particles limited the working range of the flow rate to approximately 150 μL $min^{-1}$. This is still outside the flow rate for which the specifications of the $^{1}$D quaternary pump confirm adequate gradient precision (≤0.07% RSD or 0.01 min for 0.2–5.0 mL $min^{-1}$). The resulting relative standard deviations for retention times, mainly originating from the low flow and low amounts of MP-B, were less than 5%. Yet, these slight retention time shifts frequently resulted in heart cuts beside the peak, which is a serious problem in terms of method ruggedness. Multiple optimization approaches considering re-equilibration time, the volatile additive MeOH, the dwell volume (exchange of quaternary for a binary pump) to improve the precision were undertaken without success. Increasing the flow rate was not possible due to the limiting backpressures imposed by the sub-2 μm column. Therefore, multiple other reversed phase columns were screened regarding their ability to separate the mentioned isobaric compounds. With a few exceptions, namely the Agilent Poroshell EC (150 × 3 mm, 2.7 μm) and the Waters XBridge BEH C18 (150 × 1.0 mm, 3.5 μm), with the latter having the same column chemistry as the Waters Acquity UPLC BEH C18, the majority of columns did not separate Ile, alle and Leu (Fig. 1).

Since RP chromatography follows the linear solvent strength theory, the normalized retention times between the first and last eluting compounds allowed for a good comparison of selectivities between these columns. Indeed, they differed mainly for the late eluting isobaric compounds between the Poroshell EC C18 and the BEH C18 columns (Fig. 2A). Therefore, the XBridge BEH C18 (3.5 μm) was finally selected, because it allowed a significant reduction of the operating column backpressure and thus operation at an increased flow rate. When it was used at a flow rate of 200 μL $min^{-1}$, $^{1}$D retention time precisions were below 0.25% RSD for all amino acids, which seems to be robust enough for reliable time-based multiple heart cutting 2DLC (Fig. 2B).

It should be noted that even higher $^{1}$D flowrates are disadvantageous, since decreased $^{1}$D retention times means that the $^{2}$D runs must become faster.

### 3.2. Optimization of $^{2}$D for AA analysis

The $^{2}$D separation is facing some requirements which are challenging to achieve. First of all, the $^{2}$D method must be capable to separate the enantiomers of all 19 chiral proteinogenic amino acids as well as the additionally relevant isobaric amino acids (aThr, Hse, alle, Nle, Tle) on the same column and ideally with the same mobile phase. Second, the separation must be reasonably fast so that always at least one of the 10 sampling loops of the MHC valve is available for peak storage when a new compound elutes in the $^{1}$D. This is particularly challenging in the beginning of the $^{1}$D chromatogram. In general, in heart cutting mode the speed of the $^{2}$D is less restrictive, but determines the number of cuts that can be made per unit time. The goal here was to finish the entire 2D separation in maximum 60 min. With a panel of 25 targeted amino acids it means that the $^{2}$D run time must be no longer than approximately 2 min. Unfortunately, the current software version does not allow to adjust analysis times individually for each $^{2}$D run. Hence, the strongest retained analyte dictates the acceptable $^{2}$D run time. Furthermore, mobile phase compatibility between $^{1}$D and $^{2}$D may be an issue. In chiral separation, selectivity may easily be lost if the optimal mobile phase is not employed. Furthermore, like in other modes of chromatography, peak distortion may occur due to mobile phase mismatch (the $^{1}$D mobile phase represents the sample diluent for $^{2}$D injection). For the currently evaluated QN-AX cinchonan carbamate CSP, ionic strength and possibly the water content of the $^{1}$D eluent were envisioned to be critical factors in terms of compatibility. So finally, the selection of the $^{2}$D phase system may be also driven by compatibility with the mobile phase of the $^{1}$D.

Recent studies have shown that superficially porous particle (SPP) based CSPs outperform corresponding sub-2 μm fully porous particle CSPs in terms of speed of chiral separations [54]. This can be explained by a lower total surface area per column, and also lower total porosity and column void volume, respectively. For this reason, initial experiments were employed on QN-AX SPP-based CSP, which consisted of a solid core (1.7 μm Ø) and a porous shell (0.5 μm) with 160 Å. This favorable particle morphology resulted in a gain in efficiency due to an overall improvement of the A, B and C terms in the van Deemter equation at reduced backpressures compared to sub-2 μm particle columns favorable for high speed separations at a sub-minute time scale [53,57].

The QN-AX CSP operates by an anion-exchange principle and tolerates a higher water content in the transferred fractions as long as ionic strength is lower than in the $^{2}$D eluent. The main driving force for retention is the ionic interaction between the weak anion-exchange site of the quinuclidine ring and the acidic functional group of the analyte, while additional interactions such as hydrogen-bonding between the carbamate moiety of the CSP and urea group of the AQC-tag, π-π stacking between aromatic moieties of selector and selectand, van der Waals interaction and steric hindrance caused by the *tert*-butyl motif of the selector influence both retention and chiral recognition. A prototype QN-AX core-shell CSP (3 × 50 mm, 2.7 μm) was investigated more extensively after providing more promising results in a preliminary test. Initial tests revealed that Asp, Arg, His are the critical amino acids besides the isobaric compounds of Thr and Leu, which are already separated in the $^{1}$D. Preliminary optimization was only performed with these amino acids, focusing on factors such as buffer concentration, water content, and gradient elution in the polar organic mode. The analyte retention obeys the stoichiometric displacement model and can be steered by the amount and ratio of acidic and basic additives [58,59]. With the mobile phase generally constituted of x mM $NH_4FA$ + x mM FA + 0.5% $H_2O$ in MeOH (x = 1, 2.5, 5, 10 & 50), enantioseparation increased with decreasing molarities of additives, especially for the isobaric analogues of Leu and Thr. Low molarities provided a handicap for the acidic amino acids (Glu and Asp), since retention times were too high (up to 40 min). At 50 mM they were well resolved within a short time, but enantiomers of isobaric compounds of Leu were insufficiently separated. Furthermore, Arg was unfortunately not resolved under either condition. Considering the amount of water in the mobile phase, an improved resolution of Arg and His was observed at a low water content.

Since a certain water content is inevitably introduced to the $^{2}$D depending on the elution time in the $^{1}$D, it was further investigated by injecting 20 μL of diluted aqueous sample into different mobile phases whether the water content would be tolerated. Unfortunately, no reasonable mobile phase conditions, which tolerated a transfer of the aqueous sample from $^{1}$D to $^{2}$D without loss of resolution were found for AQC-DL-Arg. Subsequently, flow rate and temperature were evaluated, resulting in 50 mM $NH_4FA$ + 50 mM FA + 0.5% $H_2O$ in MeOH, 1 mL min$^{-1}$, 30 °C as the final condition, with which all DL-enantiomers were separated within 1.5 min, except for Asp which required 2.5 min and no separation was achievable for Arg. The latter were finally resolved with a QN-AX/ZWIX tandem column approach (*vide infra*).

### 3.3. Establishing the MHC 2D-LC-QTOF MS method

The current multiple heart-cutting 2D-LC method utilized an interface with a central 2D-LC ASM valve head connected to two loop decks each carrying 6 sample storage loops á 40 μL (for details see suppl. Fig. S1). Five of the six loops of each loop deck could be used for sample storage while one loop was always reserved for the $^{1}$D mobile phase flow-through and $^{2}$D eluent, respectively. Hence, in total 10 loops were simultaneously available for fraction collection. Heart cuts taken from the first dimension were analyzed as quickly as possible in an automated manner. The system was also optimized to minimize detrimental extra-column effects. In order to prevent a loss of resolution in the $^{1}$D, the standard $^{1}$VWD with 14 μL flow cell was exchanged for a DAD with 1 μL cell, which had a beneficial effect on Rs in the $^{1}$D (see Suppl. S8). In addition, the flow path through the $^{1}$D and $^{2}$D column compartment was optimized by removal of the $^{2}$D UV detector, which resulted in a significantly improved $^{2}$D resolution (see suppl Figs. S7 and S8).

In the normal MHC mode, the first fraction was collected in loop 1 of deck A and immediately analyzed. The next cuts were stored in deck B, until the $^{2}$D was available for the analysis of the collected fractions (see Fig. S9b for a typical sampling table). In this sampling mode, the loops were filled in a consecutive order and analyzed in the reversed order, followed by a loop and transfer capillary flush to avoid carryover and contamination. During challenging separations with more than 20 cuts, it may happen that not all peaks from the $^{1}$D are collected with this sampling mode, e.g. the last peak in suppl. Fig. S9b could not be parked. A “smart peak parking” algorithm,

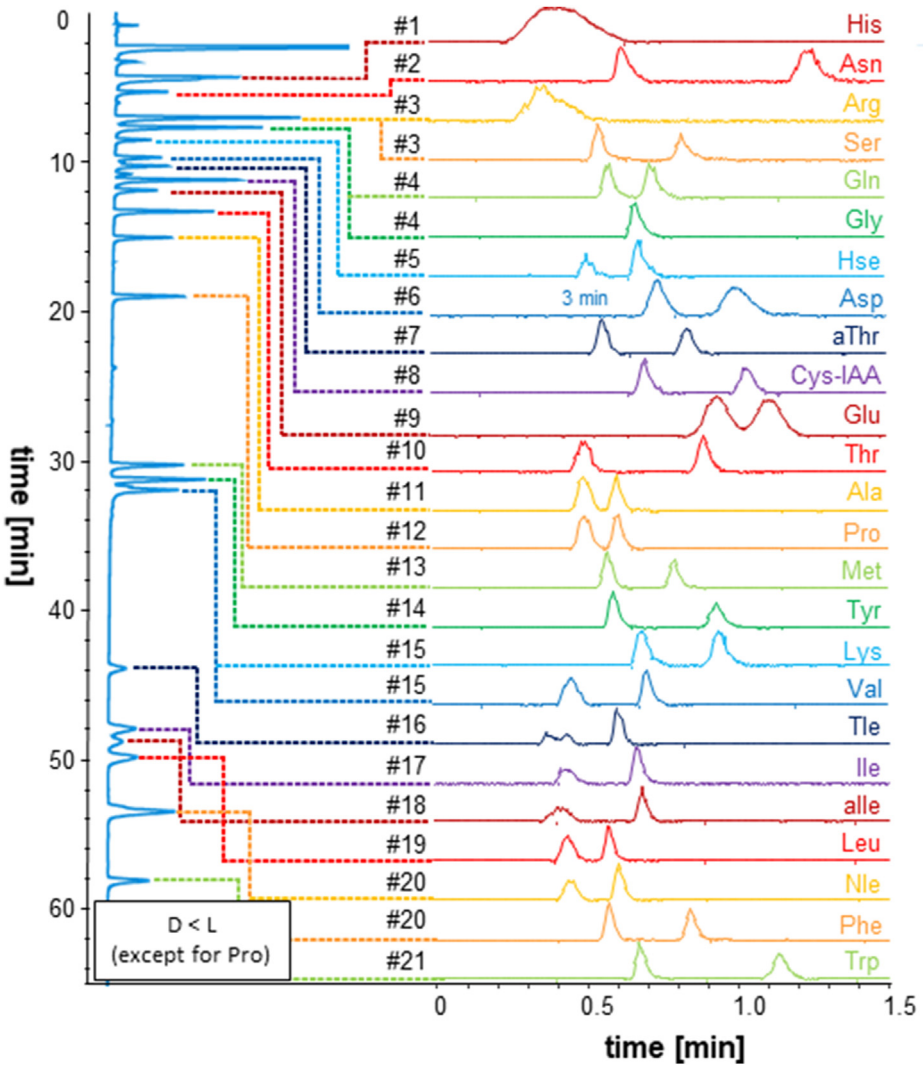


**Fig. 3.** Multiple heart cut 2D-LC analysis of 25 amino acids. Sample: 0.25 mM AA mix (25-DL-AA, 17 L-[u-$^{13}$C$^{15}$N]-AA and Cys-IAA-AQC). **$^{1}$Column**: BEH-C18 (1 × 150 mm, 1.7 μm); **$^{1}$MP-A**: 0.05% FA + 1% MeOH in water; **$^{1}$MP-B**: 0.05% FA in ACN; **$^{1}$Gradient**: 0–30 min 0–7.5% B, 30–45 min 7.5–7.5% B, 45–60 min 7.5–15% B; **$^{1}$F**: 0.15 mL min$^{-1}$; **$^{1}$T:** 50 °C, **$^{1}$Inj. vol.:** 0.5 μL, **$^{2}$Column**: QNAX core-shell (3 × 50 mm, 2.7 μm); **$^{2}$MP-A1** (isocratic): 50 mM $NH_4FA$ + 50 mM FA + 0.5% $H_2O$ in MeOH; **$^{2}$F**: 1 mL min$^{-1}$; **$^{2}$T:** 30 °C; smart peak parking.

however, does not follow the consecutive analysis order, but further optimizes the sampling and analysis procedure across both sampling decks, thereby maximizing the amount of attainable cuts (see suppl. Fig. S9a for an example and Table S5 for the final method).

Multiple heart-cutting can be performed in two sampling modes, either "time-based" or "peak-based". A time-based method places manually defined heart-cuts according to a sampling table, which is usually constructed in accordance to a $^{1}$D reference chromatogram. A peak-based method on the other hand does not need a prior run as it utilizes a predefined upslope or threshold (or a combination of both) of a peak eluting from the $^{1}$D to automatically trigger a heart cut, which requires a detector in the $^{1}$D. Each mode has its advantages and limitations. Peak based methods better cope with slight retention time shifts in the $^{1}$D which do not

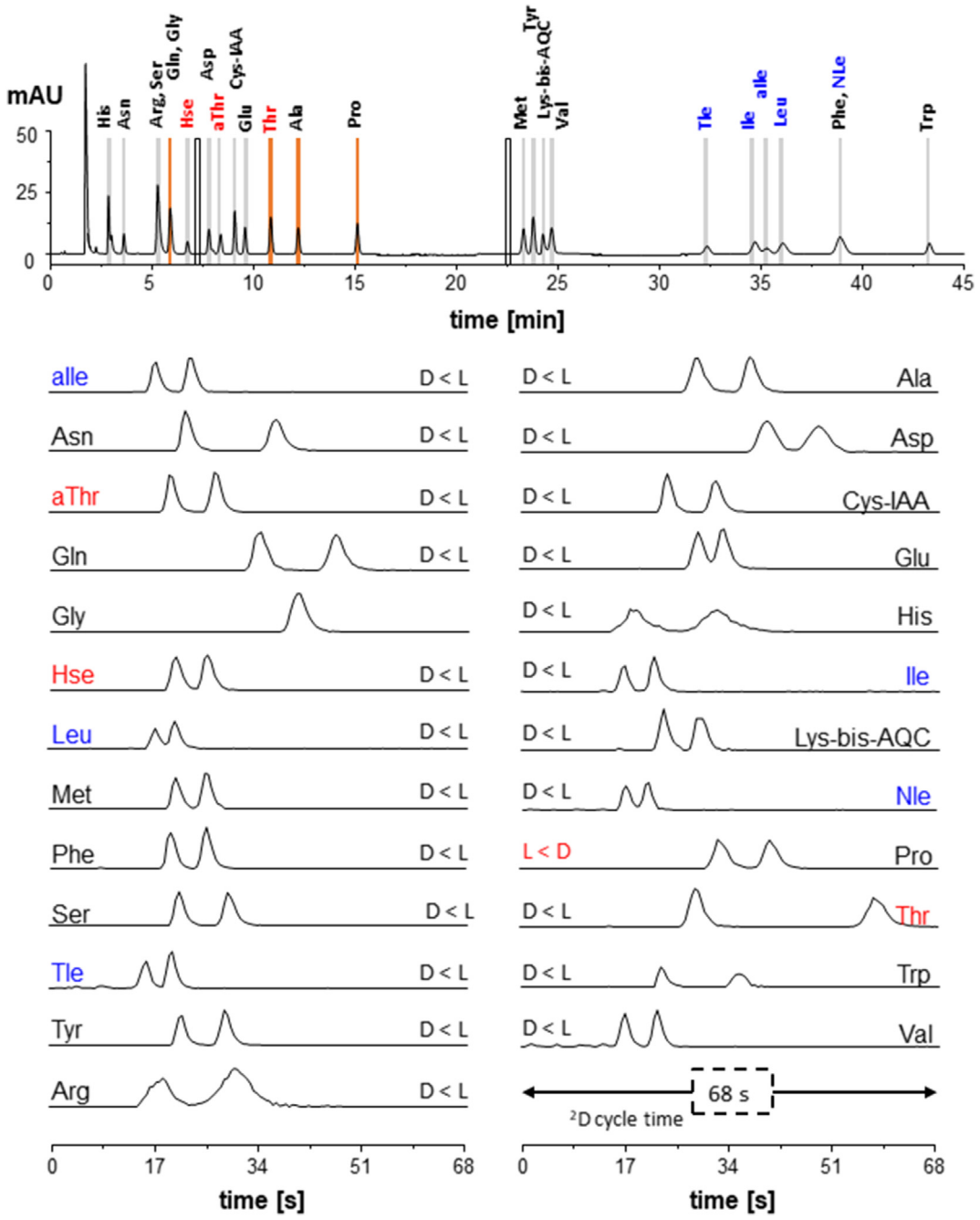


**Fig. 4.** A multiple heart cut 2D-LC analysis of 25 amino acids with tandem column in $^{2}$D. The sample contained 0.25 mM AA mix (25-DL AA, 17 L-[u-$^{13}$C$^{15}$N]-AA and Cys-IAA-AQC) separated according to the following conditions. **$^{1}$Column:** XBridge (150 × 1.0 mm, 3.5 μm); **$^{1}$MP-A:** 0.05% FA + 1% MeOH in water; **$^{1}$MP-B:** 0.05% FA in ACN; **$^{1}$Gradient:** 0–2.15 min – 0 %B, 2.15–24.65 min – 0-7.5 %B, 24.65–35.90 min – 7.5 %B, 35.90–47.15 min – 7.5–15 %B, 47.15–48.65 min – 15–50 %B, 48.65–51 min – 50 %B, 51–51.10 min – 50-0 %B, 50–65 min – 0 %B; **$^{1}$F**: 0.15 mL min$^{-1}$; **$^{1}$T:** 50 °C, **$^{1}$Inj. vol.**: 0.5 μL, **$^{2}$Column (tandem):** QNAX core-shell (3 × 50 mm, 2.7 μm)→Chiralpak ZWIX(+) FPP (3 × 20 mm, 3.0 μm).; **$^{2}$MP-A1** (isocratic)**:** 50 mM $NH_4FA$ + 50 mM FA + 0.5% $H_2O$ in MeOH (grey cuts) or **$^{2}$MP-B1** (isocratic)**:** 10 mM $NH_4FA$ + 10 mM FA + 0.5% $H_2O$ in MeOH (orange cuts); **$^{2}$F:** 2 mL min$^{-1}$; **$^{2}$T:** 30 °C; smart peak parking utilizing dummy cuts (white cuts) for equilibration of $^{2}$D. (For interpretation of the references to colour in this figure legend, the reader is referred to the Web version of this article.)

affect proper fraction transfer into the $^{2}$D. On the other hand, peaks that are not baseline resolved may not be recognized as separate peaks. If a sample contains several unexpected components and all loops are already occupied, the relevant peaks will be skipped when they elute.

In contrast to peak-based sampling, a time-based method requires a highly reproducible $^{1}$D retention time, otherwise the cut will be made "off-target". As pointed out above, in this sampling mode the advanced feature "smart peak parking" is available. It is more efficient and actually required to manage highly complex $^{1}$D chromatograms as the example in Fig. S9 shows. The resulting seemingly random parking and analysis order is recorded in a sampling table, which contains the sampling time of each loop and the subsequent analysis time in the $^{2}$D.

Fig. 3 shows the enantioselective multiple heart-cut 2D-LC-analysis of the 25 precolumn-derivatized AQC amino acids. The sampling time in the $^{1}$D was 0.2 min for all peaks. Since some critical amino acids required a low molarity of the buffer additives in the $^{2}$D, as outlined above, a "shifted step gradient" method was established in the $^{2}$D, utilizing the sampling table shown in Table S3. In fact, all separations were performed in isocratic mode (50 mM) except cuts # 4,11 and 13, which were performed with a 10 mM buffer concentration (see caption of Fig. 3). Single dummy cuts on blank $^{1}$D baseline without an analyte peak were utilized before the peak was analyzed with altered conditions to assure sufficient column equilibration. The critical peak pair Ile and alle, which would otherwise co-elute in the $^{2}$D, were resolved in the $^{1}$D. To make sure that pure fractions of these AAs are sampled, the cuts were taken at the ascending and descending parts of the Ile and alle peaks. Thus, by comparing the EICs of Leu and alle with the isotopic labelled standards of AQC-L-[u-$^{13}$C$^{15}$N]-Leu and -Ile, the peak purity of the sampled Ile and alle was confirmed (Figs. S10 and S11). This kind of flexibility cannot be realized with a peak-based method. The elution order was D < L except for Pro. Asp eluted after 3 min only, and eluted in the next chromatogram ("wrap-around") which is uncritical with MS detection. All amino acids were well resolved in enantiomer pairs, with the exception of His and Arg, which exhibit repulsive forces between their cationic side chains and the positively charged anion exchange site of the QN-AX selector.

To alleviate this problem, a tandem column approach was evaluated [15,60–62]. The 50 × 3 mm 2.7 μm QN-AX core-shell column (first column) was coupled in-line with an in-house packed 3 × 20 mm, 3.0 μm fully porous particle Chiralpak ZWIX(+) column as the second column and used for the $^{2}$D. The corresponding MHC 2D-LC enantioseparation is depicted in Fig. 4. The additional cation exchange site of the ZWIX selector provides an additional retention increment for the amino acids with cationic side chains (Arg, His) which are the most strongly retained amino acids on this column; hence their enantiomers can be well resolved. The amino acids with acidic side chains are less retained on the ZWIX column due to repulsive electrostatic interaction between their carboxylate side chain and the SCX moiety. The retention factors of the two columns in the tandem column approach is additive and due to the same stereoconfiguration of their quinine-derived selectors their relative enantiomer affinities and elution orders are the same in the two columns, allowing a full separation of all amino acids. To compensate for the longer run times with the tandem column, the flow rate was increased from 1 to 2 mL min$^{-1}$. The isobaric amino acids are depicted in blue and red. The increased $^{1}$F reduced the total analysis time to 45 min (plus 15 min re-equilibration of the $^{1}$D). Accompanied by an increased $^{2}$F, the $^{2}$D cycle time could be reduced to 68 s, without re-equilibration necessary due to the isocratic nature of the method. For Thr, Ala, Pro and Gly a lower ionic strength eluent (indicated in Fig. 4 by orange heart cuts) was used (employing 10 mM $NH_4FA$ + 10 mM FA + 0.5% $H_2O$ in MeOH instead of 50 mM $NH_4FA$ + 50 mM FA + 0.5% $H_2O$ in MeOH), which in accordance to the stoichiometric displacement model enables stronger retention in ion-exchange mode. The blank heartcuts were placed as dummy cuts to equilibrate the $^{2}$D column when the

**Table 1**
Chromatographic parameters for AQC-derivatized AAs obtained by multiple heart cutting RPLC-chiral HPLC-ESI-QTOF-MS. $^{2}$Mobile phase (isocratic): 50 mM $NH_4FA$ + 50 mM FA + 0.5% $H_2O$.

| AA-AQC | Cut # | $^{1}$D RT [min] | $^{1}$RSD (%) | $^{2}$D RT D-AAs [min] | $^{2}$RSD [%] D-AAs | $^{2}$D RT L-AAs [min] | $^{2}$RSD [%] L-AAs | Elution order | $^{2}\alpha_{DL}$ | $^{2}R_{DL}$ |
|---|---|---|---|---|---|---|---|---|---|---|
| His | 1 | 2.847 | 0.084 | 0.313 | 0.206 | 0.537 | 0.131 | D < L | 3.054 | 1.950 |
| Asn | 2 | 3.626 | 0.047 | 0.372 | 0.960 | 0.618 | 0.317 | D < L | 2.462 | 3.943 |
| Arg | 3 | 5.262 | 0.091 | 0.301 | 0.388 | 1.509 | 0.187 | D < L | 13.395 | 9.315 |
| Ser | 3 | 5.262 | 0.091 | 0.353 | 0.192 | 0.489 | 0.000 | D < L | 1.910 | 2.533 |
| Gln[a] | 4 | 5.896 | 0.060 | 0.574 | 0.000 | 0.783 | 0.166 | D < L | 1.564 | 2.812 |
| Gly[a] | 4 | 5.896 | 0.060 | 0.680 | 0.038 | – | – | – | – | – |
| Hse | 5 | 6.762 | 0.141 | 0.322 | 0.098 | 0.401 | 0.056 | D < L | 1.671 | 1.537 |
| Asp | 7 | 7.361 | 0.140 | 0.665 | 0.085 | 0.806 | 0.049 | D < L | 1.306 | 1.391 |
| aThr | 8 | 8.348 | 0.149 | 0.335 | 0.042 | 0.457 | 0.042 | D < L | 1.929 | 2.420 |
| Cys-IAA | 9 | 9.058 | 0.108 | 0.401 | 0.275 | 0.533 | 0.062 | D < L | 1.672 | 2.488 |
| Glu | 10 | 9.574 | 0.078 | 0.485 | 0.059 | 0.552 | 0.000 | D < L | 1.238 | 1.100 |
| Thr[a] | 11 | 10.863 | 0.077 | 0.478 | 0.195 | 0.969 | 0.031 | D < L | 2.789 | 5.997 |
| Ala[a] | 12 | 12.215 | 0.079 | 0.481 | 0.088 | 0.628 | 0.033 | D < L | 1.531 | 2.232 |
| Pro[a] | 13 | 15.105 | 0.070 | 0.681 | 0.141 | 0.544 | 0.035 | L < D | 1.403 | 1.881 |
| Met | 15 | 23.317 | 0.204 | 0.341 | 0.398 | 0.427 | 0.442 | D < L | 1.629 | 1.740 |
| Tyr | 16 | 23.795 | 0.078 | 0.356 | 0.095 | 0.477 | 0.024 | D < L | 1.796 | 2.436 |
| Lys-bis-AQC | 17 | 24.277 | 0.102 | 0.388 | 0.362 | 0.488 | 0.341 | D < L | 1.543 | 1.730 |
| Val | 18 | 24.707 | 0.097 | 0.280 | 0.357 | 0.369 | 0.388 | D < L | 2.168 | 1.912 |
| Tle | 21 | 32.359 | 0.122 | 0.262 | 0.044 | 0.332 | 0.033 | D < L | 2.208 | 1.465 |
| Ile | 23 | 34.688 | 0.097 | 0.282 | 0.015 | 0.365 | 0.015 | D < L | 2.062 | 1.852 |
| alle | 25 | 35.261 | 0.089 | 0.292 | 0.016 | 0.389 | 0.032 | D < L | 2.108 | 2.013 |
| Leu | 26 | 36.056 | 0.084 | 0.289 | 0.023 | 0.343 | 0.000 | D < L | 1.635 | 1.160 |
| Phe | 28 | 38.916 | 0.074 | 0.332 | 0.014 | 0.429 | 0.000 | D < L | 1.755 | 1.967 |
| Nle | 28 | 38.916 | 0.074 | 0.287 | 0.014 | 0.346 | 0.038 | D < L | 1.707 | 1.306 |
| Trp | 30 | 43.267 | 0.036 | 0.376 | 0.035 | 0.585 | 0.034 | D < L | 2.212 | 3.385 |

[a] $^{2}$Mobile phase (isocratic): 10 mM $NH_4FA$ + 10 mM FA + 0.5% $H_2O$.

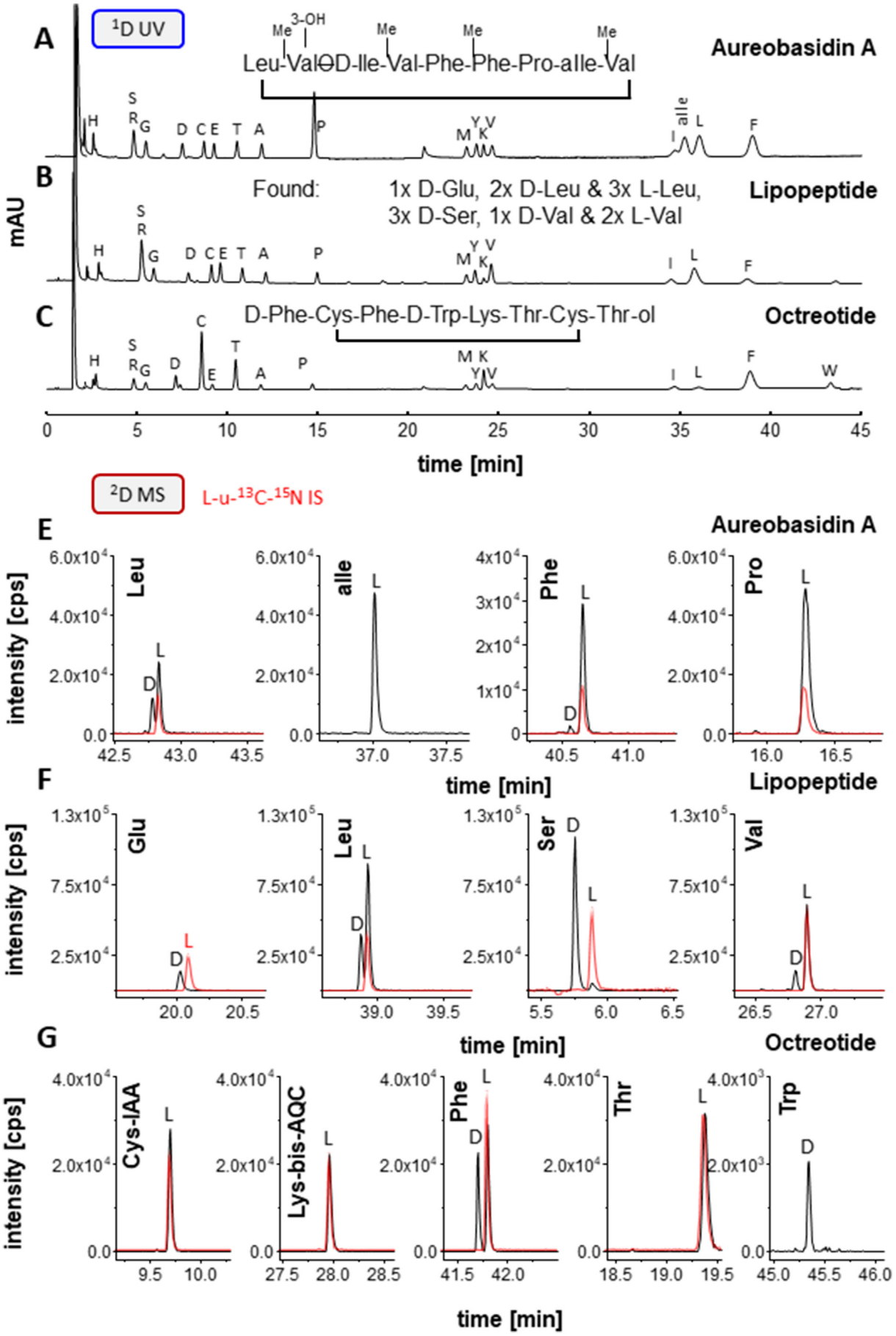


**Fig. 5.** Applied multiple heart cutting 2D-LC for Aureobasidin A, a lipopeptide research sample and Octreotide. The corresponding $^{1}$D UV chromatograms (**A**, **B**, **C**) and the corresponding $^{2}$D XICs of the identified AAs (**D**, **E**, **F**) are depicted, respectively. All proteinogenic AAs (except Trp, Gln and Asn) were included as L-[u-$^{13}$C$^{15}$N] internal standard for reference.

mobile phase conditions change (note, the analysis order of the dummy cuts does not correspond to the position in the $^{1}$D chromatogram due to the smart peak parking algorithm). The full sampling table of this optimized method can be found in Suppl. Table S3. Table 1 summarizes the chromatographic data of the $^{1}$D and $^{2}$D along with run-to-run repeatability (n = 3). It can be seen that the precision of $^{1}$D retention time was always <0.21% RSD and that of the $^{2}$D typically <0.4% RSD. All amino acids are fully baseline resolved (except Leu and Glu with Rs 1.1) which indicates the practical suitability for applications in AA stereoconfiguration determination of peptide hydrolysates. Although being not of relevance in the current application, LODs were estimated to be around 1.11 nM (which corresponds to 0.111 pmol injected on-column in the $^{1}$D or 0.055 pmol per enantiomer peak in the $^{2}$D).

Comparable 2D-LC methods perform inferior in either analysis time, maximum number of surveilled amino acids or both. Hamase et al. typically utilize more than 2 h for selected amino acids at a time, nonetheless with the advantage of quantitative sampling and an increased avoidance of matrix interferences from real samples [21,30,63]. Similarly, in an achiral-chiral approach Woiwode et al. [42] and Ianni et al. [22] were unable to resolve the isobaric compounds Ile, Leu, and alle in the achiral dimension, with analysis times of >115 min for 16 AAs and 130 min for 22 AAs, respectively. In a 1D approach, Kimura et al. [15] and Horak et al. [14] managed the separation of all proteinogenic amino acids (including alle and aThr) within 60 min on a coupled QN-AX/ZWIX(+) and ZWIX(+) CSP, respectively, unfortunately without the resolution of D-lle and D-alle, which is the main drawback. Amino acid enantioseparation using GC–MS on Chirasil L-Val as the state of the art remains a valuable alternative, whereby enantiomers of Leu, Ile and alle can be well resolved but other amino acids are problematic such as Arg, His and Cys [5,64].

### 3.4. Application for the elucidation of absolute configurations in peptides

The assignment of the absolute configurations of the amino acid constituents is an integral part of the structure elucidation of novel peptides from the natural pool as well as in quality control of the stereointegrity of therapeutic and synthetic peptides, respectively. For this purpose, peptide hydrolysis was performed according to the European Pharmacopoeia 10.0 in order to release the free amino acids for subsequent enantioselective MHC 2D-LC amino acid analysis.

#### 3.4.1. Aureobasidin

Aureobasidin A, a cyclic depsipeptide with antifungal activity, was chosen as an exemplary L-alle containing peptide (Fig. S12). Besides, the peptide hydrolysate should contain a number of proteinogenic amino acids (L-Leu, L-Pro, and L-Phe) as well as special amino and hydroxy acids (*N*-methyl-L-valine, *N*-methyl-L-phenylalanine, 2-(*R*)-hydroxy-3-(*R*)-methylpentanoic acid, β-hydroxy-*N*-methyl-L-valine) (which were not in the focus herein) [65,66]. The experimental results (Fig. 5E) indeed reveal the presence of L-alle L-Leu, L-Pro, and L-Phe. However, also D-Leu and a small quantity of D-Phe were found which might result from peptide impurities in aureobasidin A (see Fig. S12) [66]. Note, only the targeted 25 amino acids were transferred from the $^{1}$D to the $^{2}$D for MS detection, therefore *N*-methylated and hydroxylated AAs were not analyzed. These uncommon amino acids, however, could be targeted in an adjusted MHC method.

#### 3.4.2. Lipopeptide

Lipopeptides are produced by certain bacteria strains that frequently contain a significant percentage of D-amino acids (which protect them from enzymatic digestion) and very often non-proteinogenic AAs such as alle. The optimized enantioselective MHC-2DLC amino acid analysis method was implemented for the qualitative analysis of a novel lipopeptide following acidic hydrolysis.

According to genome sequencing and NMR data [67], the cyclic peptide moiety contained Glu, Leu, Ser, Val, but their ratio and stereoconfiguration was unknown. The $^{1}$D UV chromatogram of the sample including internal standards is shown in Fig. 5B. It turned out that no alle was present in this lipopeptide, however, a number of D-amino acids were confirmed. The L-configured isotopically labelled internal standards allowed a clear identification between the D- and L-isomers, and the area ratios allowed the determination of the number of the respective amino acid in the peptide. From the chromatogram shown in Fig. 5F it can be seen that the analyzed lipopeptide research sample is constituted of 1x D-Glu, 2x D-Leu, 3x L-Leu, 3x D-Ser, 1x D-Val and 2x L-Val. However, the actual peptide sequence within the cyclic peptide has yet to be elucidated, by utilizing a different approach that preserves the amino acid connectivity [5].

#### 3.4.3. Octreotide

A further example was the analysis of the hydrolysate from the cyclic therapeutic peptide Octreotide, which is a synthetic analog of the peptide hormone somatostatin. Its C-terminal Thr is reduced to an alcohol and the ring closure is obtained by a disulfide bridge between two Cys residues. The synthetic peptide contains two D-amino acids, i.e. one D-Trp and one D-Phe. The EICs of all expected amino acids Cys-IAA, Lys-bis-AQC, Phe, Thr and Trp are shown in Fig. 5G. It becomes evident that the current Octreotide sample has correct stereochemical integrity. Trp was present only in D-form, Phe as 1:1 mixture of D and L, while the other amino acids (Cys, Lys, Thr) were present in L-form only. The configuration of threaninol must be analyzed by a different method.

## 4. Conclusion

A targeted enantioselective MHC 2D-LC-ESI-QTOF-MS amino acid analysis method was established for the simultaneous enantioseparation of all proteinogenic amino acids, including the side chain isomeric analogues of Leu (alle, Nle, Tle), and Thr (aThr, Hse) (in total 25 components), within a total runtime of 45 min (including re-equilibration 65 min). The $^{1}$D achiral RPLC separation resolved the majority of amino acids from each other and from their isomeric analogues which could not be separated simultaneously by the $^{2}$D chiral separation. Particularly challenging was the separation of alle and Ile, besides Leu, in the $^{1}$D, but was finally accomplished on an XBridge BEH C18 column. Complete enantioseparation of all 24 chiral amino acids was achieved by constructing a robust $^{1}$D achiral separation (RSD of retention times < 0.21%, n = 3) utilizing a tandem column approach with a 2.7 μm QNAX core-shell column (5 cm long) and a short 3 μm FFP ZWIX(+) column (2 cm long) in the $^{2}$D for fast enantiomer separation of the AQC-amino acids in less than 68 s. The AQC tag not only provided a chromophor and fluorophor, but also an easily ionizable mass tag allowing highly selective and sensitive MS detection. The achiral pre-separation not only ensured proper separation of the isobaric amino acids, but may be beneficial if a more complex matrix is present, reducing bias from matrix effects. The automated MHC 2D-LC setup can be applied for the quality control of the integrity of the stereochemistry of amino acid constituents in therapeutic peptides and structural elucidation of the configurations in natural (lipo-/cyclo-)peptides. Similar MHC-2D-LC methods can be developed with little adaptations for other analytes and could be particularly valuable for chiral drugs with multiple chiral centers.

## CRediT authorship contribution statement

**Ryan Karongo:** Investigation, Methodology, Formal analysis, Data curation, Visualization, Writing – original draft, Writing – review & editing. **Min Ge:** Investigation, Methodology, Formal analysis, Data curation, Writing – review & editing. **Christian Geibel:** Investigation, Writing – review & editing. **Jeannie Horak:** Conceptualization, Methodology, Supervision, Writing – review & editing. **Michael Lämmerhofer:** Conceptualization, Methodology, Supervision, Writing – review & editing, Resources, Funding acquisition.

## Declaration of competing interest

The authors declare that they have no known competing financial interests or personal relationships that could have appeared to influence the work reported in this paper.

## Acknowledgements

We are grateful to Agilent Technologies for support of this research by an Agilent Research Award (#4068). The authors thank Dr. Stephan Buckenmaier from Agilent Technologies, Waldbronn, Germany, for technical advice and valuable discussions.

## Appendix A. Supplementary data

Supplementary data to this article can be found online at https://doi.org/10.1016/j.aca.2021.338858.

## References

[1] P.M. Masters, J.L. Bada, J. Samuel Zigler, Aspartic acid racemisation in the human lens during ageing and in cataract formation, Nature 268 (5615) (1977) 71–73.
[2] M.G. Friedrich, S.E. Hancock, M.J. Raftery, R.J.W. Truscott, Isoaspartic acid is present at specific sites in myelin basic protein from multiple sclerosis patients: could this represent a trigger for disease onset? Acta Neuropathologica Communications 4 (1) (2016) 83.
[3] T.R. Lambeth, D.L. Riggs, L.E. Talbert, J. Tang, E. Coburn, A.S. Kang, J. Noll, C. Augello, B.D. Ford, R.R. Julian, Spontaneous isomerization of long-lived proteins provides a molecular mechanism for the lysosomal failure observed in Alzheimer's disease, ACS Cent. Sci. 5 (8) (2019) 1387–1395.
[4] M. D'Hondt, N. Bracke, L. Taevernier, B. Gevaert, F. Verbeke, E. Wynendaele, B. De Spiegeleer, Related impurities in peptide medicines, J. Pharmaceut. Biomed. Anal. 101 (2014) 2–30.
[5] H. Gerhardt, A. Sievers-Engler, G. Jahanshah, Z. Pataj, F. Ianni, H. Gross, W. Lindner, M. Lämmerhofer, Methods for the comprehensive structural elucidation of constitution and stereochemistry of lipopeptides, J. Chromatogr. A 1428 (2016) 280–291.
[6] E. Bayer, H. Allmendinger, G. Enderle, B. Koppenhoefer, Anwendung von d-Chirasil-Val bei der gas-chromatographischen Analytik von Enantiomeren, Fresenius' Z. für Anal. Chem. 321 (4) (1985) 321–324.
[7] V. Schurig, Separation of enantiomers by gas chromatography, J. Chromatogr. A 906 (1) (2001) 275–299.
[8] B. Koppenhoefer, V. Muschalek, M. Hummel, E. Bayer, Determination of the enhancement of the enantiomeric purity during recrystallization of amino acids, J. Chromatogr. A 477 (1) (1989) 139–145.
[9] Z. Dai, Z. Wu, S. Jia, G. Wu, Analysis of amino acid composition in proteins of animal tissues and foods as pre-column o-phthaldialdehyde derivatives by HPLC with fluorescence detection, J. Chromatogr. B 964 (2014) 116–127.
[10] S. Sethi, J. Martens, R. Bhushan, Assessment and application of Marfey's reagent and analogs in enantioseparation: a decade's perspective, Biomed. Chromatogr. 35 (1) (2021), e4990.
[11] I. Ilisz, A. Péter, W. Lindner, State-of-the-art enantioseparations of natural and unnatural amino acids by high-performance liquid chromatography, Trac. Trends Anal. Chem. 81 (2016) 11–22.
[12] S. Ferre, V. Gonzalez-Ruiz, D. Guillarme, S. Rudaz, Analytical strategies for the determination of amino acids: past, present and future trends, J Chromatogr B Analyt Technol Biomed Life Sci 1132 (2019) 121819.
[13] S. Tanwar, R. Bhushan, Enantioresolution of amino acids: a decade's perspective, prospects and challenges, Chromatographia 78 (17) (2015) 1113–1134.
[14] J. Horak, M. Lämmerhofer, Stereoselective separation of underivatized and 6-aminoquinolyl-N-hydroxysuccinimidyl carbamate derivatized amino acids using zwitterionic quinine and quinidine type stationary phases by liquid chromatography-High resolution mass spectrometry, J. Chromatogr. A 1596 (2019) 69–78, https://doi.org/10.1016/j.chroma.2019.02.060.
[15] R. Kimura, H. Tsujimura, M. Tsuchiya, S. Soga, N. Ota, A. Tanaka, H. Kim, Development of a cognitive function marker based on D-amino acid proportions using new chiral tandem LC-MS/MS systems, Sci. Rep. 10 (1) (2020) 804.
[16] S. Du, Y. Wang, C.A. Weatherly, K. Holden, D.W. Armstrong, Variations of l- and d-amino acid levels in the brain of wild-type and mutant mice lacking d-amino acid oxidase activity, Anal. Bioanal. Chem. 410 (12) (2018) 2971–2979.
[17] K. Yoshikawa, M. Furuno, N. Tanaka, E. Fukusaki, Fast enantiomeric separation of amino acids using liquid chromatography/mass spectrometry on a chiral crown ether stationary phase, J. Biosci. Bioeng. 130 (4) (2020) 437–442.
[18] J. Horak, M. Lämmerhofer, Derivatize, racemize, and analyze—an easy and simple procedure for chiral amino acid standard preparation for enantioselective metabolomics, Anal. Chem. 91 (12) (2019) 7679–7689, https://doi.org/10.1021/acs.analchem.9b00666.
[19] R. Hellinger, J. Horak, W. Lindner, Enantioseparation of 6-aminoquinolyl-N-hydroxysuccinimidyl carbamate tagged amino acids and other zwitterionic compounds on cinchona-based chiral stationary phases, Anal. Bioanal. Chem. 405 (25) (2013) 8105–8120.
[20] A. Acquaviva, G. Siano, P. Quintas, M.R. Filgueira, C.B. Castells, Chiral x Achiral Multidimensional Liquid Chromatography. Application to the enantioseparation of dintitrophenyl amino acids in honey samples and their fingerprint classification, J. Chromatogr. A 1614 (2019), 460729.
[21] C. Ishii, T. Akita, M. Mita, T. Ide, K. Hamase, Development of an online two-dimensional high-performance liquid chromatographic system in combination with tandem mass spectrometric detection for enantiomeric analysis of free amino acids in human physiological fluid, J. Chromatogr. A 1570 (2018) 91–98.
[22] F. Ianni, R. Sardella, A. Lisanti, A. Gioiello, B.T. Cenci Goga, W. Lindner, B. Natalini, Achiral–chiral two-dimensional chromatography of free amino acids in milk: a promising tool for detecting different levels of mastitis in cows, J. Pharmaceut. Biomed. Anal. 116 (2015) 40–46.
[23] X. Yao, T.T.Y. Tan, Y. Wang, Thiol–ene click chemistry derived cationic cyclodextrin chiral stationary phase and its enhanced separation performance in liquid chromatography, J. Chromatogr. A 1326 (2014) 80–88.
[24] I. Molnár-Perl, Advancement in the derivatizations of the amino groups with the o-phthaldehyde-thiol and with the 9-fluorenylmethyloxycarbonyl chloride reagents, J. Chromatogr. B 879 (17) (2011) 1241–1269.
[25] U. Woiwode, R.J. Reischl, S. Buckenmaier, W. Lindner, M. Lämmerhofer, Imaging peptide and protein chirality via amino acid analysis by chiral × chiral two-dimensional correlation liquid chromatography, Anal. Chem. 90 (13) (2018) 7963–7971, https://doi.org/10.1021/acs.analchem.8b00676.
[26] G. Mazzoccanti, S. Manetto, A. Ricci, W. Cabri, A. Orlandin, M. Catani, S. Felletti, A. Cavazzini, M. Ye, H. Ritchie, C. Villani, F. Gasparrini, High–throughput enantioseparation of Nα–fluorenylmethoxycarbonyl proteinogenic amino acids through fast chiral chromatography on zwitterionic-teicoplanin stationary phases, J. Chromatogr. A 1624 (2020) 461235.
[27] E.L. Regalado, C.J. Welch, Separation of achiral analytes using supercritical fluid chromatography with chiral stationary phases, Trac. Trends Anal. Chem. 67 (2015) 74–81.
[28] J.M. Will, A. Behrens, M. Macke, C.D. Quarles, U. Karst, Automated chiral analysis of amino acids based on chiral derivatization and trapped ion mobility–mass spectrometry, Anal. Chem. 93 (2) (2021) 878–885.
[29] R. Pérez-Míguez, B. Bruyneel, M. Castro-Puyana, M.L. Marina, G.W. Somsen, E. Domínguez-Vega, Chiral discrimination of DL-amino acids by trapped ion mobility spectrometry after derivatization with (+)-1-(9-Fluorenyl)ethyl chloroformate, Anal. Chem. 91 (5) (2019) 3277–3285.
[30] C. Ishii, A. Furusho, C.-L. Hsieh, K. Hamase, Multi-dimensional high-performance liquid chromatographic determination of chiral amino acids and related compounds in real world samples, Chromatography 41 (1) (2020) 1–17.
[31] Y. Miyoshi, K. Hamase, Y. Tojo, M. Mita, R. Konno, K. Zaitsu, Determination of d-serine and d-alanine in the tissues and physiological fluids of mice with various d-amino-acid oxidase activities using two-dimensional high-performance liquid chromatography with fluorescence detection, J. Chromatogr. B 877 (24) (2009) 2506–2512.
[32] K.J. Adams, B. Pratt, N. Bose, L.G. Dubois, L. St John-Williams, K.M. Perrott, K. Ky, P. Kapahi, V. Sharma, M.J. MacCoss, M.A. Moseley, C.A. Colton, B.X. MacLean, B. Schilling, J.W. Thompson, Skyline for small molecules: a unifying software package for quantitative metabolomics, J. Proteome Res. 19 (4) (2020) 1447–1458.
[33] J. Lin, C. Tsang, R. Lieu, K. Zhang, Method screening strategies of stereoisomers of compounds with multiple chiral centers and a single chiral center, J. Chromatogr. A 1624 (2020) 461244.
[34] M.P. Dwight Stoll, Stephan Buckenmaier, 2D-LC - A Tutorial Focusing on Best Practices, HPLC Milano, 2019.
[35] D.R. Stoll, P.W. Carr, Two-dimensional liquid chromatography: a state of the art tutorial, Anal. Chem. 89 (1) (2017) 519–531.
[36] P. Dugo, F. Cacciola, T. Kumm, G. Dugo, L. Mondello, Comprehensive multidimensional liquid chromatography: theory and applications, J. Chromatogr. A 1184 (1) (2008) 353–368.
[37] A.F.G. Gargano, M. Duffin, P. Navarro, P.J. Schoenmakers, Reducing dilution and analysis time in online comprehensive two-dimensional liquid

chromatography by active modulation, Anal. Chem. 88 (3) (2016) 1785–1793.
[38] B.W.J. Pirok, D.R. Stoll, P.J. Schoenmakers, Recent developments in two-dimensional liquid chromatography: fundamental improvements for practical applications, Anal. Chem. 91 (1) (2019) 240–263.
[39] H. Wang, H.R. Lhotka, R. Bennett, M. Potapenko, C.J. Pickens, B.F. Mann, I.A.H. Ahmad, E.L. Regalado, Introducing online multicolumn two-dimensional liquid chromatography screening for facile selection of stationary and mobile phase conditions in both dimensions, J. Chromatogr. A 1622 (2020) 460895.
[40] M. Pursch, S. Buckenmaier, Loop-based multiple heart-cutting two-dimensional liquid chromatography for target analysis in complex matrices, Anal. Chem. 87 (10) (2015) 5310–5317.
[41] M. Pursch, P. Lewer, S. Buckenmaier, Resolving Co-elution problems of components in complex mixtures by multiple heart-cutting 2D-LC, Chromatographia 80 (1) (2017) 31–38.
[42] U. Woiwode, S. Neubauer, W. Lindner, S. Buckenmaier, M. Lämmerhofer, Enantioselective multiple heartcut two-dimensional ultra-high-performance liquid chromatography method with a Coreshell chiral stationary phase in the second dimension for analysis of all proteinogenic amino acids in a single run, J. Chromatogr. A 1562 (2018) 69–77.
[43] N. Grecsó, M. Kohout, A. Carotti, R. Sardella, B. Natalini, F. Fülöp, W. Lindner, A. Péter, I. Ilisz, Mechanistic considerations of enantiorecognition on novel Cinchona alkaloid-based zwitterionic chiral stationary phases from the aspect of the separation of trans-paroxetine enantiomers as model compounds, J. Pharmaceut. Biomed. Anal. 124 (2016) 164–173.
[44] I. Ilisz, A. Bajtai, W. Lindner, A. Péter, Liquid chromatographic enantiomer separations applying chiral ion-exchangers based on Cinchona alkaloids, J. Pharmaceut. Biomed. Anal. 159 (2018) 127–152.
[45] U. Woiwode, M. Ferri, N.M. Maier, W. Lindner, M. Lämmerhofer, Complementary enantioselectivity profiles of chiral cinchonan carbamate selectors with distinct carbamate residues and their implementation in enantioselective two-dimensional high-performance liquid chromatography of amino acids, J. Chromatogr. A 1558 (2018) 29–36.
[46] K. Hamase, A. Morikawa, T. Ohgusu, W. Lindner, K. Zaitsu, Comprehensive analysis of branched aliphatic d-amino acids in mammals using an integrated multi-loop two-dimensional column-switching high-performance liquid chromatographic system combining reversed-phase and enantioselective columns, J. Chromatogr. A 1143 (1) (2007) 105–111.
[47] Y. Tojo, K. Hamase, M. Nakata, A. Morikawa, M. Mita, Y. Ashida, W. Lindner, K. Zaitsu, Automated and simultaneous two-dimensional micro-high-performance liquid chromatographic determination of proline and hydroxyproline enantiomers in mammals, J. Chromatogr. B 875 (1) (2008) 174–179.
[48] H. Han, Y. Miyoshi, K. Ueno, C. Okamura, Y. Tojo, M. Mita, W. Lindner, K. Zaitsu, K. Hamase, Simultaneous determination of d-aspartic acid and d-glutamic acid in rat tissues and physiological fluids using a multi-loop two-dimensional HPLC procedure, J. Chromatogr. B 879 (29) (2011) 3196–3202.
[49] G. Lajkó, I. Ilisz, G. Tóth, F. Fülöp, W. Lindner, A. Péter, Application of Cinchona alkaloid-based zwitterionic chiral stationary phases in supercritical fluid chromatography for the enantioseparation of Nα-protected proteinogenic amino acids, J. Chromatogr. A 1415 (2015) 134–145.
[50] P.A. Levkin, N.M. Maier, V. Schurig, W. Lindner, Strong detrimental effect of a minute enantiomeric impurity of a chiral selector on the enantioselectivity factor, Angew. Chem. Int. Ed. 49 (42) (2010) 7742–7744.
[51] M. Wolter, M. Lämmerhofer, In-situ functionalized monolithic polysiloxane-polymethacrylate composite materials from polythiol-ene double click reaction in capillary column format for enantioselective nano-high-performance liquid chromatography, J. Chromatogr. A 1497 (2017) 172–179.
[52] S. Karakawa, K. Shimbo, N. Yamada, T. Mizukoshi, H. Miyano, M. Mita, W. Lindner, K. Hamase, Simultaneous analysis of d-alanine, d-aspartic acid, and d-serine using chiral high-performance liquid chromatography-tandem mass spectrometry and its application to the rat plasma and tissues, J. Pharmaceut. Biomed. Anal. 115 (2015) 123–129.
[53] C. Geibel, K. Dittrich, U. Woiwode, M. Kohout, T. Zhang, W. Lindner, M. Lammerhofer, Evaluation of superficially porous particle based zwitterionic chiral ion exchangers against fully porous particle benchmarks for enantioselective ultra-high performance liquid chromatography, J. Chromatogr. A 1603 (2019) 130–140, https://doi.org/10.1016/j.chroma.2019.06.026.
[54] K. Schmitt, U. Woiwode, M. Kohout, T. Zhang, W. Lindner, M. Lämmerhofer, Comparison of small size fully porous particles and superficially porous particles of chiral anion-exchange type stationary phases in ultra-high performance liquid chromatography: effect of particle and pore size on chromatographic efficiency and kinetic performance, J. Chromatogr. A 1569 (2018) 149–159, https://doi.org/10.1016/j.chroma.2018.07.056.
[55] C.V. Hoffmann, R. Pell, M. Lämmerhofer, W. Lindner, Synergistic effects on enantioselectivity of zwitterionic chiral stationary phases for separations of chiral acids, bases, and amino acids by HPLC, Anal. Chem. 80 (22) (2008) 8780–8789.
[56] I. Molnar, Computerized design of separation strategies by reversed-phase liquid chromatography: development of DryLab software, J. Chromatogr. A 965 (1) (2002) 175–194.
[57] R. Hayes, A. Ahmed, T. Edge, H. Zhang, Core–shell particles: preparation, fundamentals and applications in high performance liquid chromatography, J. Chromatogr. A 1357 (2014) 36–52.
[58] M. Lämmerhofer, W. Lindner, Liquid chromatographic enantiomer separation and chiral recognition by cinchona alkaloid-derived enantioselective separation materials, Adv. Chromatogr. 46 (2008) 1–107.
[59] M. Lämmerhofer, Chiral recognition by enantioselective liquid chromatography: mechanisms and modern chiral stationary phases, J. Chromatogr. A 1217 (6) (2010) 814–856.
[60] I. D'Acquarica, F. Gasparrini, B. Giannoli, E. Badaloni, B. Galletti, F. Giorgi, M.O. Tinti, A. Vigevani, Enantio- and chemo-selective HPLC separations by chiral–achiral tandem-columns approach: the combination of CHIROBIOTIC TAG™ and SCX columns for the analysis of propionyl carnitine and related impurities, J. Chromatogr. A 1061 (2) (2004) 167–173.
[61] R. Sardella, M. Lämmerhofer, B. Natalini, W. Lindner, In-line coupling of a reversed-phase column to cope with limited chemoselectivity of a quinine carbamate-based anion-exchange type chiral stationary phase, J. Separ. Sci. 31 (10) (2008) 1702–1711.
[62] R.S. Hegade, M. De Beer, F. Lynen, Chiral stationary phase optimized selectivity liquid chromatography: a strategy for the separation of chiral isomers, J. Chromatogr. A 1515 (2017) 109–117.
[63] C. Ishii, T. Akita, M. Nagano, M. Mita, K. Hamase, Determination of chiral amino acids in various fermented products using a two-dimensional HPLC-MS/MS system, Chromatography 40 (2) (2019) 83–87.
[64] J. Horak, H. Gerhardt, J. Theiner, W. Lindner, Correlation between amino acid racemization and processing conditions for various wheat products, oil seed press cakes and lignin samples, Food Bioprod. Process. 92 (4) (2014) 355–368.
[65] K.T. Katsushige Ikail, Kazuro Shiomi, Makoto Moriguchi, Yoshihisa Umeda, Junko Yamamoto, Ikunoshin Kato, Hiroshi Naganawa, Structure of aureobasidin A, J. Antibiot. 44 (9) (1991) 925–933.
[66] Y. In, T. Ishida, K. Takesako, Unique molecular conformation of aureobasidin A, a highly amide N-methylated cyclic depsipeptide with potent antifungal activity: X-ray crystal structure and molecular modeling studies, J. Pept. Res. 53 (5) (1999) 492–500.
[67] H. Gross, V.O. Stockwell, M.D. Henkels, B. Nowak-Thompson, J.E. Loper, W.H. Gerwick, The genomisotopic approach: a systematic method to isolate products of orphan biosynthetic gene clusters, Chem. Biol. 14 (1) (2007) 53–63.